Recent progress of the tiled-grating research

Yanlei Zuo (左言磊)[1,2], Xiaofeng Wei (魏晓峰)[1], Qihua Zhu (朱启华)[1], Xiao Wang (王 逍)[1], Wei Han (韩 伟)[1], Zheng Huang (黄 征)[1], Hongjie Liu (刘红婕)[1], and Chuntong Ying (应纯同)[2]

[1]*Research Center of Laser Fusion, China Academy of Engineering Physics, Mianyang 6219002*

[2]*Department of Engineering Physics, Tsinghua University, Beijing 100084*

In this article, we present some new progress in the tiled-grating field which mainly includes the theoretical description of all the errors existing in the tiled-grating system and the experimental setup used to eliminate the errors.

OCIS codes: 050.1590, 050.2770, 060.4510.

In usual chirped pulse amplification (CPA) laser systems, the energy scale is limited by the size of its compressor containing a grating pair with a limited damage threshold[1,2]. The critical compressor component is the last grating which experiences the shortest pulse and therefore the highest power. However, the difficult fabrication process may limit the ultimate size of individual grating to less than 1 m[3,4]. As proposed by Zhang *et al.*[5], the coherent summation of multiple gratings to form a larger grating provides an alternative to larger-sized diffraction grating.

Theoretical and experimental studies about grating tiling have been carried out. Zhang *et al.*[5] presented a design criterion by limiting the stretch of the pulse from a tiled-grating compressor (TGC). Zeng *et al.*[6] limited the lateral and longitudinal phase errors in a very small scale by using a two-color heterodyne interferometer. Kessler *et al.*[7] have demonstrated subpicosecond-pulse compression and achieved Fourier-transform-limited pulses by use of tiled gratings.

However, the analysis made by Zhang *et al.*[5] is aiming at an ordinary compressor, not a TGC, because the focal spot will break up evidently due to the phase error before the duration of the output pulse from a TGC is impacted. A theory based on the interference between beams in their far field is put forward and a detailed TGC is introduced in this article.

The physical model we investigate is shown in Fig. 1. In a TGC, the first grating G1 is individual while the last grating comprises two gratings G2A and G2B. We assume in the next discussion that misalignment exist only in G2A. Propagating through the TGC, a beam splits into two coherent sub-beams experiencing different temporal and spatial modulations. Coherent addition of the two sub-beams occurs in the focal plane of an ideal lens.

As shown in Fig. 2, there are six errors between the two tiled gratings affecting the optical performance of a TGC defined as $d\theta_x$ (rotation about x axis), $d\theta_y$ (rotation about y axis), $d\theta_z$ (rotation about z axis), dx (translation in x axis), dz (translation in z axis), and Δd (error in line frequency). All the errors above can be divided into two kinds which are translation and rotation errors. The former, including the tip, tilt, twist and groove-width errors, causes deflection while the latter, including the shift and piston errors, causes phase delay between the two sub-beams from the TGC.

Phase delay occurs when the shift and piston errors exist in a tiled-grating system, the shift and piston errors can be described as

$$\phi_s = \frac{\Delta s}{d} \cdot 2\pi,$$
$$\phi_p = \frac{\Delta p}{\lambda} \cdot (\cos\alpha(\omega) + \cos\beta) \cdot 2\pi, \qquad (1)$$

where Δs and Δp are the values of the shift and piston errors, respectively, d is groove width of the grating, λ is the wavelength, α and β are the incidence and diffraction angles, respectively.

It is known that the two errors cause deflection of the beam in the x-z plane in Fig. 1. Denoting the deflection angle as ε_x, we can express the angle as

$$\varepsilon_{x1} \cong \frac{\Delta d}{d^2} \cdot \frac{\lambda}{\cos\beta},$$
$$\varepsilon_{x2} \cong \Delta\xi(1 + \frac{\cos\alpha(\omega)}{\cos\beta}), \qquad (2)$$

where ε_{x1} and ε_{x2} are caused by the groove-width error and tilt error, respectively, Δd and $\Delta\xi$ are the values of the groove-width error and the tilt error, respectively.

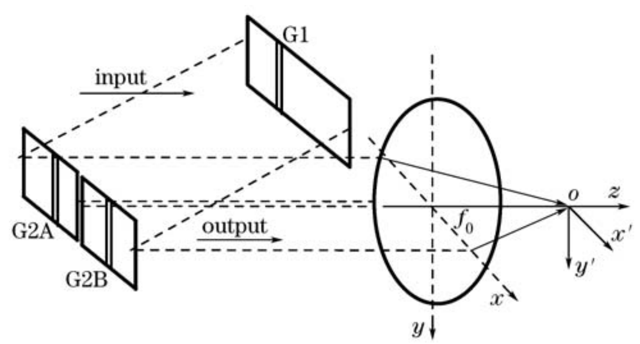

Fig. 1. Chirped pulse passing through a TGC and an ideal lens.

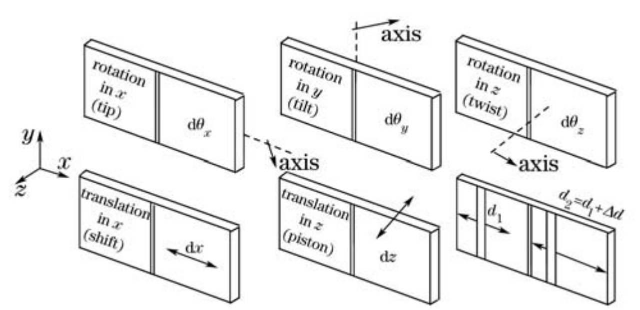

Fig. 2. Errors in a tiled-grating system.

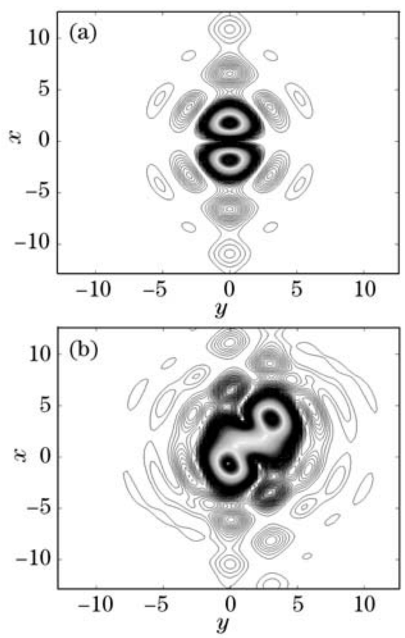

Fig. 3. Distribution of the far field for (a) phase delay of π and (b) $\varepsilon_x \neq 0$, $\varepsilon_y \neq 0$.

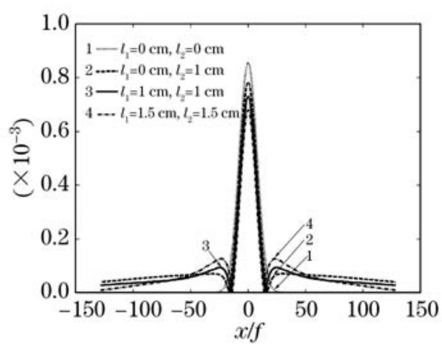

Fig. 4. Far-field distribution considering the seam effect between the tiled gratings.

The two errors cause beam deflection in the y-z plane in Fig. 1, which can be expressed by

$$\varepsilon_{y1} \approx \Delta\delta \cdot (\sin\alpha(\omega) + \sin\beta),$$
$$\varepsilon_{y2} \approx \Delta\zeta \cdot (\cos\alpha(\omega) + \cos\beta), \tag{3}$$

where ε_{y1} and ε_{y2} are the deflection angles by the twist and tip error, respectively, $\Delta\delta$ and $\Delta\zeta$ are the values of the twist and tip errors, respectively.

What the researchers in the field concern is the far-field properties of the output pulse from the TGC, therefore some numerical calculation is carried out for the distribution in the far field, which is listed as follows.

Figure 3 shows that only π phase delay is large enough to split the focal spot into two halves and a little rotation error can make the two focal spots of the sub-beams apart from each other.

In an actual tile-grating system, the seam between the two tile gratings is not neglectable as we deal with above, because the is diffracted by the seam during its passing through the TGC. Figure 4 shows the far-field distribution of a beam through a single-pass TGC where each grating comprises two small gratings. From Fig. 4, two side wings scale as the width of the seam increases, so the existence of the seam make the focal spot less concentrated. The effect of the seam on the temporal property of the output pulse is also considered, numerical simulation of which shows that the impact is of a scale of a few percent.

It is very difficult to implement the alignment in six degrees of freedom, so a scheme of error compensation in pair is put forward where the coherent addition of the sub-beams is realized though each error is nonzero. In the scheme, the shift and piston errors, the tilt and groove-width errors, the twist and tip errors are compensated by each other, respectively. However, the compensation between the errors is aiming at the central wavelength only, which will cause temporal broadening of the output pulse from a TGC. Results of numerical simulation are shown for a TGC system with an aperture of 20 cm as follows.

Figure 5 shows that the effect of temporal broadening becomes more and more serious with the increase of the spectral width of the chirped pulse for compression.

Figure 6 is the experimental test bed for the demonstration of pulse compression by a tiled-grating compressor. The single-pass pulse compressor comprises G1 and G2, spaced by 2.4 m. The beam deflection angle at the gratings is set to 7.4 degrees. The grating G2 contains two small gratings G2a and G2b.

The gold-coated gratings in the experiment have a line frequency of 1700/mm and a clear aperture of 180×110 (mm). The beam diameters of the operation laser and probe laser are limited to 80 mm because of the small-sized gratings.

A method which is based on the far-field diagnostics completely is developed for the alignment of the two tiled

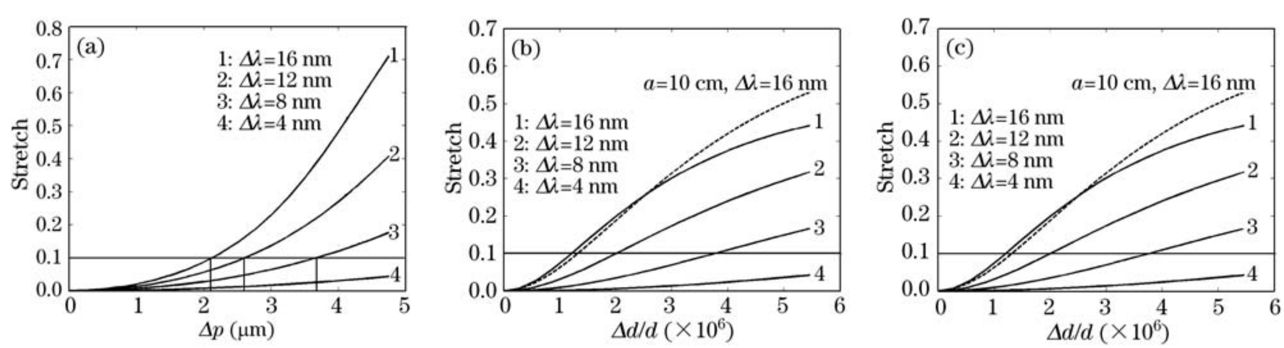

Fig. 5. Temporal stretch for mutual compensation of (a) piston and shift errors, (b) tilt and groove-width errors, (c) twist and tip errors.

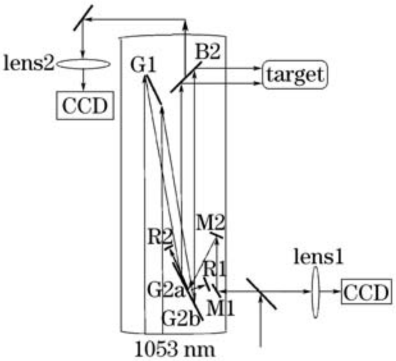

Fig. 6. Detailed schematic of the experimental test bed.

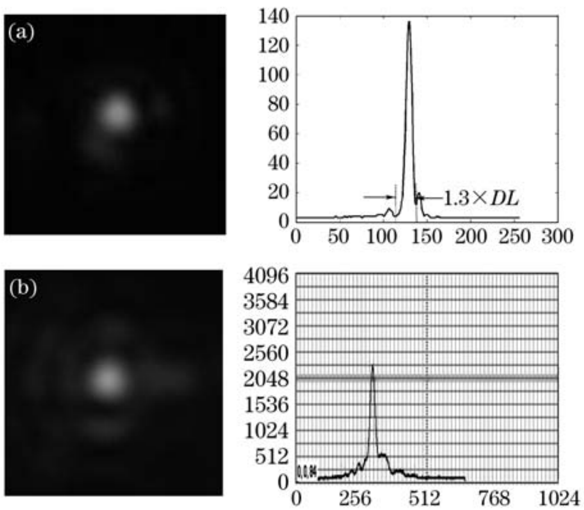

Fig. 7. Far-field distribution after alignment for (a) the operation laser and (b) the probe laser.

gratings. For the first time as far as we know the real-time monitoring of the tiled gratings for the final-use angle of 1053-nm chirped pulse is implemented for two gratings with different line frequencies, as shown in Fig. 7, where the far field of the operation laser appears as a single focal spot only if the two tiled gratings are well aligned by the probe laser. A simple but very effective method is developed for the elimination of the longitudinal piston error from about 10 to 0.1 μm. For improvement of the system's stability, a flexible material is used and the effect is remarkable. After the alignment is finished, the tiled-grating system is relatively stable, so we cannot achieve an absolutely stable focal spot.

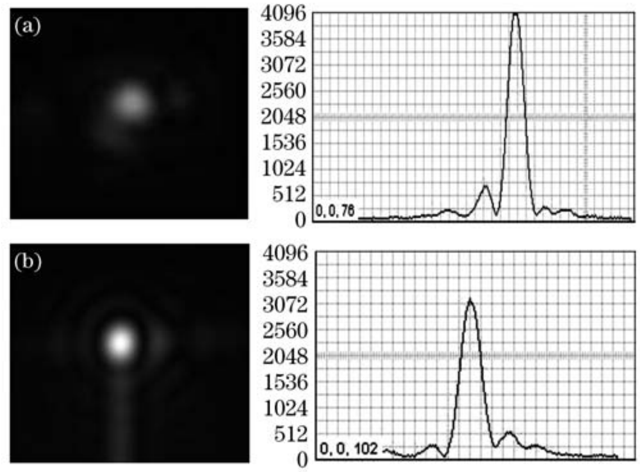

Fig. 8. Focal spot's departure from the Airy spot with a side wing (a) in the left and (b) in the right.

During the course of the variation of the focal spot's shape, two focal spots which have the maximal departure from the perfect airy spot with their intensity distribution in the direction of the focal spot's splitting are captured as shown in Fig. 8.

Some theoretical results are shown in the article, including the effects of all the errors on the far field of the output pulse and the impacts of compensation in pair on the temporal property. Experimental setup is introduced and some new progress in experiment are presented.

This work was supported by the Key Laboratory Program on High Temperature and High Density Plasmas Physics under Grant No. 9140c6803010702. Y. Zuo's e-mail address is zuoyanlei@tsinghua.org.cn.

References

1. M. D. Perry and G. Mourou, Science **264,** 917 (1994).
2. D. M. Penningtong, C. G. Brown, T. E. Cowan, and H. P. Hatchett, IEEE J. Sel. Top. Quantum Electron. **6,** 676 (2000).
3. L. Li and J. Hirsh, Opt. Lett. **20,** 1349 (1995).
4. B. W. Shore and M. D. Perry, J. Opt. Soc. Am. A **14,** 1124 (1997).
5. T. Zhang, M. Yonemura, and Y. Kato, Opt. Commun. **145,** 367 (1998).
6. L. Zeng and L. Li, Opt. Lett. **31,** 152 (2006).
7. T. J. Kessler, J. Bunkenburg, H. Huang, A. Kozlov, and D. D. Meyerhofer, Opt. Lett. **29,** 635 (2004).